Wind shear effects on cloud-radiation feedback in the western Pacific warm pool

Jia-Lin Lin and Brian Mapes

Climate Diagnostics Center, Cooperative Institute for Research in Environmental Sciences, NOAA, Boulder, Colorado, USA

Received 7 April 2004; revised 18 July 2004; accepted 5 August 2004; published 31 August 2004.

[1] Upper tropospheric stratiform clouds associated with deep convection are important to global radiation budgets and to cloud-radiation feedbacks on climate variability and change. Several recent observational studies indicate that vertical wind shear is an important factor affecting stratiform cloud fraction and cloud overlap. This study further examines wind shear effects on cloud properties (including cloud fraction and cloud optical depth) and associated top of atmosphere (TOA) and surface radiative fluxes, using observations from the Tropical Ocean Global Atmosphere program's Coupled Ocean Atmosphere Response Experiment (TOGA COARE) experiment and long-term satellite measurements. Wind shear affects cloud-radiative fluxes, through both the cloud fraction and optical thickness, in a strong and systematic way. In typical convecting conditions, shear-induced additional cloudiness can reduce outgoing longwave radiation (OLR) by 10s of Wm^{-2}, implying longwave radiative changes on the order of 10% of the total latent heating. Such cloud also reflects shortwave radiation, reducing surface downward flux (energy input to the ocean) by 10s of Wm^{-2}. Current climate models lack these effects. *INDEX TERMS:* 3314 Meteorology and Atmospheric Dynamics: Convective processes; 3359 Meteorology and Atmospheric Dynamics: Radiative processes; 3374 Meteorology and Atmospheric Dynamics: Tropical meteorology; 0320 Atmospheric Composition and Structure: Cloud physics and chemistry. **Citation:** Lin, J.-L., and B. Mapes (2004), Wind shear effects on cloud-radiation feedback in the western Pacific warm pool, *Geophys. Res. Lett.*, *31*, L16118, doi:10.1029/2004GL020199.

1. Introduction

[2] Cloud radiation feedback is well recognized as a key uncertainty in predicting any potential future climate change [*Intergovernmental Panel on Climate Change*, 2001]. The upper tropospheric stratiform clouds (anvil and cirrus clouds) associated with tropical deep convection are important to the earth's radiation budgets because of their large longwave (LW) and shortwave (SW) cloud radiative forcing (CRF [*Ramanathan et al.*, 1989] Interestingly, the seasonal-mean LW CRF and SW CRF nearly cancel each other in current climate, but this delicate balance between two big terms is sensitive to the stratiform cloud properties, and breaking of the balance is observed when stratiform cloud properties change, for example, during a strong El Niño event [*Cess et al.*, 2001], and in the tropical intraseasonal oscillation [*Lin and Mapes*, 2004]. Climate change modeling studies also show that, in different models, changes in stratiform cloud properties lead to different changes in LW CRF and SW CRF, because of their associated cloud fraction feedback [e.g., *Hansen et al.*, 1984] and cloud optical depth feedback (e.g., *Charlock* [1982]; *Somerville and Remer* [1984]; see review by *Del Genio and Wolf* [2000]).

[3] Although the SW CRF and LW CRF nearly cancel, SW cooling acts mainly at the surface while LW warming acts mainly on the atmosphere. The surface SW cooling is important for regulating the tropical sea surface temperature [e.g., *Ramanathan and Collins*, 1991]. The atmospheric LW warming, together with vertical gradients in its heating profile [e.g., *Webster and Stephens*, 1980; *Ackerman et al.*, 1988], play an important role in tropical large-scale circulations such as the Hadley circulation [e.g., *Randall et al.*, 1989], the Walker circulation [e.g., *Bretherton and Sobel*, 2002] and the tropical intraseasonal oscillation [e.g., *Lin and Mapes*, 2004]. Therefore, parameterization of stratiform clouds is an important aspect of General Circulation Models (GCMs).

[4] The art of cloud parameterization in GCMs has evolved steadily in complexity from prescribed cloud properties, to diagnostic schemes, to prognosed schemes (see reviews by *Randall* [1989] and *Fowler et al.* [1996]). Current schemes often use prognostic equations to predict various cloud and precipitation variables (such as cloud ice, rain, or snow), and include parameterizations of a large number of microphysical pathways between these categories. After that, fractional cloudiness can be predicted using either the diagnostic method (see review by *Xu and Krueger* [1991]) or the statistical method (see review by *Tompkins* [2002]). The predictors often employed are grid-scale thermodynamical and microphysical properties, such as relative humidity, total water content, convective mass flux, large-scale mass flux, and precipitation.

[5] In addition to the grid-scale thermodynamical and microphysical properties, observations indicate that vertical wind shear is another important factor affecting stratiform cloud fraction [*Saxen and Rutledge*, 2000] and cloud overlap characteristics [*Mace and Benson-Troth*, 2002; *Hogan and Illingworth*, 2003], yet shear dependence is not included in any climate model we know of, and evidently doesn't arise automatically (Figure 7).

[6] When evaluating a satellite rainfall retrieval algorithm using data from TOGA COARE, *Saxen and Rutledge* [2000] found that for a given rainrate, the coverage of cold clouds (with cloud top temperature < 235 K or cloud top pressure < 275 hPa) increases with vertical wind shear. Using cloud radar data from a midlatitude station, *Hogan and Illingworth* [2003] found that strong wind shear

0094-8276/04/2004GL020199$05.00

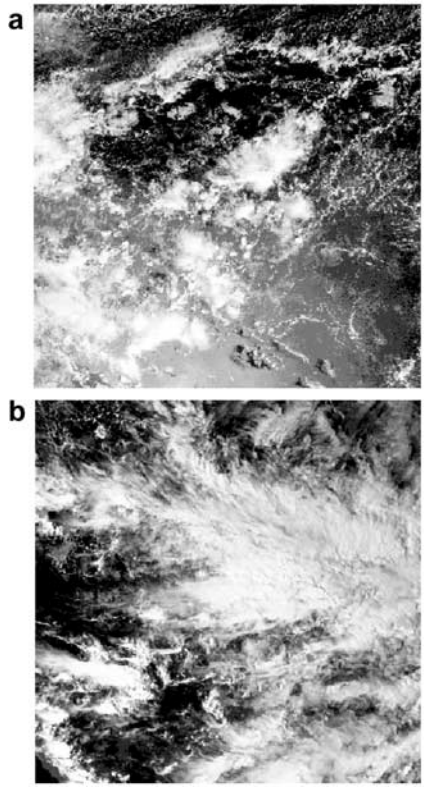

Figure 1. Visible images from GMS-4 for (a) December 9, 1992 at 00:03 UTC, and (b) February 13, 1993 at 05:03 UTC. The region is between 10N–10S and 145E–165E centered on the TOGA COARE Intensive Flux Array (IFA). The IFA mean surface rainrate, estimated by a composite of two shipborne radars, is 0.25 mm/hr for both cases. The 150–700 hPa shear is 6.2 m/s for (a) but 34.4 m/s for (b).

decreases the correlation length of clouds between different vertical levels, suggesting that wind shear decreases the cloud overlap and hence increases total cloud cover.

[7] As an example, visible satellite images for two scenes with similar mean rainrate (as estimated either from radar or from heat and moisture budgets) but quite different vertical wind shear are shown in Figure 1. The strong shear case (Figure 1b) is clearly associated with more cirrus coverage than the weak shear case (Figure 1a). In addition to this increased thin cirrus cloud, precipitating stratiform clouds also contribute a larger fraction of total rainfall in conditions of stronger shear [e.g., *Lin et al.*, 2004].

[8] The above studies serve to raise the following questions:

[9] (1) How much does the wind shear affect the total cloud fraction and cloud top height, which is important for the cloud fraction feedback?

[10] (2) Does the wind shear also affect the cloud optical depth?

[11] (3) Is the wind shear effect detectable in the associated radiative fluxes?

[12] The purpose of this study is to address the above questions using observations from the TOGA COARE experiment and long-term satellite measurements. Datasets used are described in section 2. The wind shear effects are analyzed in section 3. Summary and discussions are given in section 4.

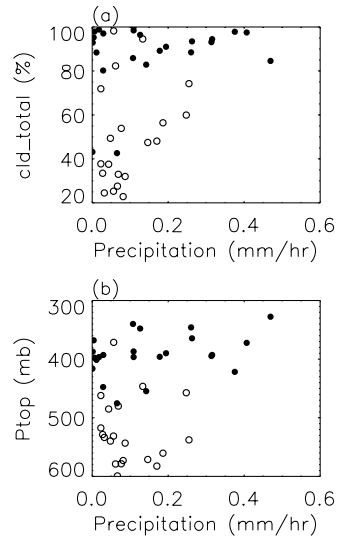

Figure 2. Scatter diagram of TOGA COARE IFA daily-mean radar-estimated rainrate versus (a) ISCCP total cloud fraction, and (b) ISCCP averaged cloud top pressure. Open circles are for the lower quartile of 150–700 hPa wind shear, while filled circles are for the upper quartile.

2. Data

[13] Datasets used in this study include TOGA COARE data and long-term satellite data. The variables used include clouds, radiative fluxes, surface precipitation, and wind profiles.

[14] The TOGA COARE data are area-averages for the Intensive Flux Array (IFA) covering the 4-month period from November 1992 to February 1993. The clouds come from the 3-hourly International Satellite Cloud Climatology Project (ISCCP) D1 data [*Rossow and Schiffer*, 1999]; The TOA and surface radiative fluxes come from the 3-hourly data by *Krueger and Burks* [1998], with the TOA fluxes from the GMS-derived broadband fluxes [*Minnis et al.*, 1995], and the surface fluxes from averages of measurements at five surface stations. The surface precipitation comes from the 10-minute radar-estimated rainfall map [*Short et al.*, 1997], which cover about 60% of the IFA area. The wind profiles come from the 6-hourly upper air soundings [*Ciesielski et al.*, 2002]. All datasets are averaged to daily data and we use only the days without any missing data. The long-term measurements are 15 years (1979–

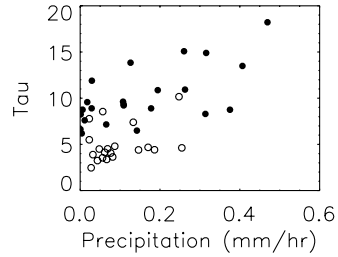

Figure 3. As in Figure 2 except for ISCCP averaged cloud optical depth.

1993) of daily mean (5475 days) OLR from Advanced Very High Resolution Radiometer (AVHRR [*Liebmann and Smith*, 1996]), precipitation from Microwave Sounding Units (MSU) [*Spencer*, 1993], and wind profiles from the NCEP/NCAR reanalysis [*Kalnay et al.*, 1996]. We use the data averaged over a 10 degree by 10 degree region (5N–5S, 150–160E) in the western Pacific warm pool, which covers the TOGA COARE IFA.

3. Wind Shear Effects on Clouds and Radiative Fluxes

[15] First we consider wind shear effects on the TOGA COARE IFA clouds and radiation fluxes. We stratify the data by the strength of 150–700 hPa wind shear, and compare the lower and upper quartiles. Figure 2a shows the scatter diagram of ISCCP total cloud fraction versus radar-estimated rainrate. The weak shear quartile (open circles) and strong shear quartile (filled circles) appear as distinct regimes. For a given value of rainrate, strong shear increases the cloud fraction by more than 20%. The increase is mainly in high and middle clouds (not shown), resulting in an increase of averaged cloud top height (Figure 2b). Besides increasing the cloud fraction and cloud top height, wind shear also increases the cloud optical depth (Figure 3).

[16] The effects of shear on stratiform cloud properties should be detectable in the associated radiative fluxes. To test this possibility, Figure 4 shows the scatter diagram of GMS-derived broadband OLR versus rainrate. As expected, OLR generally decreases (note inverted scale of y axis) with increased rainrate. However, for a given value of rainrate, strong wind shear decreases the OLR by 10s of Wm^{-2}, implying a radiative heating difference in the atmosphere which is more than 10% of the total latent heating for a moderate area-averaged rainrate of 0.3 mm/hr.

[17] In addition to the LW effect, wind shear also increases the TOA reflected SW flux by 10s of Wm^{-2} (Figure 5a), and decreases the downward SW flux at the ocean's surface, which is measured by independent ground-based instruments (Figure 5b by a similar amount).

[18] Comparison of Figure 4 and Figure 5a indicates that the shear-induced changes in TOA OLR and reflected SW flux largely cancel out. Therefore, the effect of shear is to repartition radiative heating between the atmosphere and the ocean, not to change the overall column radiative heating.

[19] Although a systematic relationship is clearly indicated by Figure 4 and Figure 5, the TOGA COARE data provide a too small sample for reliable quantitative assessment. To bolster the case, we also analyzed the long-term measurements of OLR from AVHRR, precipitation from MSU, and wind profiles from NCEP/NCAR reanalysis. The resulting joint dependence, binned into a 5 × 5 array of precipitation and shear categories, is shown in Figure 6. Contours slope up to the left, indicating that OLR decreases both with increased rainrate and with increased wind shear. For a given value of rainrate, strong shear reduces the OLR by about 20 Wm^{-2}, which is consistent with the TOGA COARE results (Figure 4).

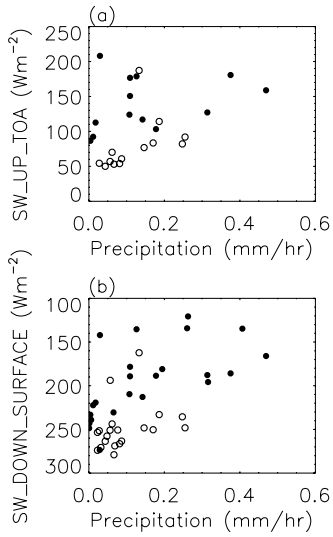

Figure 5. As in Figure 2 except for (a) GMS-derived broadband TOA reflected SW flux, and (b) surface downward SW flux from average of five surface stations.

[20] Next we compare the observational results with a climate model – the NCAR Community Atmosphere Model CAM2, which uses a prognostic cloud microphysics scheme [*Rasch and Kristjansson*, 1998] and cirrus cloud fraction proportional to convective mass flux [*Collins et al.*, 2000]. We used four years (1985–1988) of daily mean (1460 days) outputs from an AMIP-type simulation. The data were averaged along the equator (between 5N and 5S) with a zonal resolution of 10 degree longitude. To make the sample size comparable to that of the above long-term observational data, we used five 10 degree by 10 degree grids from 130E to 180E in the western Pacific warm pool. Figure 7 shows that, in contrast with observation (Figure 6), the CAM2 OLR does not change substantially with vertical wind shear.

4. Summary and Discussions

[21] In summary, wind shear strongly affects cloud-radiative fluxes, through both the cloud fraction and optical

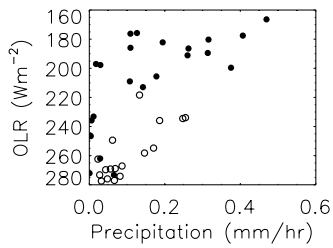

Figure 4. As in Figure 2 except for GMS-derived broadband OLR.

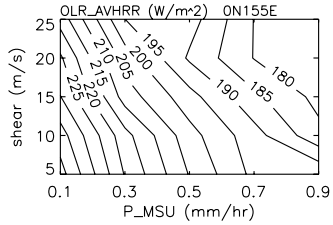

Figure 6. Variation of AVHRR OLR as a function of MSU precipitation and NCEP 200–850 hPa wind shear.

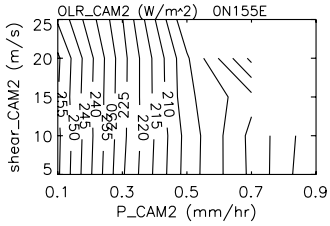

Figure 7. As in Figure 6 except for outputs from NCAR CAM2.

thickness. The effect is strong and systematic, with wind shear reducing OLR by 10s of Wm^{-2}, implying radiative changes on the order of 10% of the total latent heating. Shear-induced cloud also reflects SW radiation, reducing surface downward flux (energy input to the ocean) by 10s of Wm^{-2}.

[22] Our results raise the following questions for future studies:

[23] (1) What are the physical mechanisms behind the wind shear effect? Is it mainly due to increased cloud cover at one level or decreased cloud overlap between different levels? What causes the increase of cloud optical depth?

[24] (2) What are the impacts of the shear effect on climate and climate change?

[25] We plan to study these questions using more detailed long-term observations from the Atmospheric Radiation Measurement (ARM) sites, and outputs from GCM experiments.

[26] **Acknowledgments.** This study benefits from the discussions with Chris Bretherton, Dick Johnson, Dave Randall and Ed Zipser. Steve Krueger kindly provided the TOGA COARE radiative fluxes data. Jim Hurrell and Adam Phillips kindly provided the NCAR CAM2 outputs. The research described here was supported by NSF grants ATM-0336790, ATM-0097116 and ATM-0112715, and by NOAA OGP CMEP.

References

Ackerman, T. P., K.-N. Liou, F. P. J. Valero, and L. Pfister (1988), Heating rates in tropical anvils, *J. Atmos. Sci.*, *45*, 1606–1623.

Bretherton, C. S., and A. H. Sobel (2002), A simple model of a convectively coupled walker circulation using the weak temperature gradient approximation, *J. Clim.*, *15*, 2907–2920.

Cess, R. D., M. H. Zhang, B. A. Wielicki, D. F. Young, X.-L. Zhou, and Y. Nikitenko (2001), The influence of the 1998 El Niño upon cloud-radiative forcing over the Pacific warm pool, *J. Clim.*, *14*, 2129–2137.

Charlock, T. P. (1982), Cloud optical feedback and climate stability in a radiative-convective model, *Tellus*, *34*, 245–254.

Ciesielski, P. E., R. H. Johnson, and J. Wang (2002), Impacts of humidity-corrected sonde data on TOGA COARE analyses, paper presented at 25th Conference on Hurricanes and Tropical Meteorology, Am. Metereol. Soc., San Diego, Calif.

Collins, W. D., et al. (2000), Description of the NCAR Community Atmosphere Model (CAM2), *NCAR/TN-464+STR*, 190 pp., Natl. Cent. for Atmos. Res., Boulder, Colo.

Del Genio, A. D., and A. B. Wolf (2000), The temperature dependence of the liquid water path of low clouds in the southern Great Plains, *J. Clim.*, *13*, 3465–3486.

Fowler, L. D., D. A. Randall, and S. A. Rutledge (1996), Liquid and ice cloud microphysics in the CSU general circulation model. Part I: Model description and simulated microphysical processes, *J. Clim.*, *9*, 489–529.

Hansen, J., A. Lacis, D. Rind, G. Russell, P. Stone, I. Fung, R. Ruedy, and J. Lerner (1984), Climate sensitivity: Analysis of feedback mechanisms, in *Climate Processes and Climate Sensitivity*, *Geophys. Monogr. Ser.*, vol. 29, edited by J. E. Hanson and T. Takahashi, pp. 130–163, AGU, Washington, D. C.

Hogan, R. J., and A. J. Illingworth (2003), Parameterizing ice cloud inhomogeneity and the overlap of inhomogeneities using cloud radar data, *J. Atmos. Sci.*, *60*, 756–767.

Intergovernmental Panel on Climate Change (2001), *Climate Change 2001: The Scientific Basis: Contribution of Working Group I to the Third Assessment Report of the Intergovernmental Panel on Climate Change*, edited by J. T. Houghton et al., 892 pp., Cambridge Univ. Press, New York.

Kalnay, E., et al. (1996), The NCEP/NCAR 40-year reanalysis project, *Bull. Am. Meteorol. Soc.*, *77*, 437–472.

Krueger, S. K., and J. E. Burks (1998), Radiative fluxes and heating rates during TOGA COARE over the intensive flux array, paper presented at CLIVAR/GEWEX COARE98 Conference, Natl. Inst. of Stand. and Technol., Boulder, Colo.

Liebmann, B., and C. A. Smith (1996), Description of a complete (interpolated) outgoing longwave radiation dataset, *Bull. Am. Meteorol. Soc.*, *77*, 1275–1277.

Lin, J. L., and B. E. Mapes (2004), Radiation budget of the tropical intraseasonal oscillations, *J. Atmos. Sci.*, *61*, 2050–2062.

Lin, J. L., B. E. Mapes, M. H. Zhang, and M. Newman (2004), Stratiform precipitation, vertical heating profiles, and the Madden-Julian Oscillation, *J. Atmos. Sci.*, *61*, 296–309.

Mace, G. G., and S. Benson-Troth (2002), Cloud-layer overlap characteristics derived from long-term cloud radar data, *J. Clim.*, *15*, 2505–2515.

Minnis, P., W. L. Smith Jr., D. P. Garber, J. K. Ayers, and D. R. Doelling (1995), Cloud properties derived from GOES-7 for the spring 1994 ARM intensive observing period using version 1.0.0 of the ARM satellite data analysis program, *NASA Rep. 1366*, 59 pp.

Ramanathan, V., and W. Collins (1991), Thermodynamic regulation of ocean warming by cirrus clouds deduced from observations of the 1987 El Niño, *Nature*, *351*, 27–32.

Ramanathan, V., R. D. Cess, E. F. Harrison, P. Minnis, B. R. Barkstrom, E. Ahmad, and D. Hartmann (1989), Cloud-radiative forcing and climate: Results from the Earth Radiation Budget experiment, *Science*, *243*, 57–63.

Randall, D. A. (1989), Cloud parameterization for climate models: Status and prospects, *Atmos. Res.*, *23*, 341–361.

Randall, D. A., Harshvardhan, D. A. Dazlich, and T. G. Cosetti (1989), Interactions among radiation, convection, and large-scale dynamics in a general circulation model, *J. Atmos. Sci.*, *46*, 1943–1970.

Rasch, P. J., and J. E. Kristjansson (1998), A comparison of the CCM3 model climate using diagnosed and predicted condensate parameterizations, *J. Clim.*, *11*, 1587–1614.

Rossow, W. B., and R. A. Schiffer (1999), Advances in understanding clouds from ISCCP, *Bull. Am. Meteorol. Soc.*, *80*, 2261–2288.

Saxen, T. R., and S. A. Rutledge (2000), Surface rainfall-cold cloud fractional coverage relationship in TOGA COARE: A function of vertical wind shear, *Mon. Weather Rev.*, *128*, 407–415.

Short, D. A., P. A. Kucera, B. S. Ferrier, J. C. Gerlach, S. A. Rutledge, and O. W. Thiele (1997), Shipboard radar rainfall patterns within the TOGA COARE IFA, *Bull. Am. Meteorol. Soc.*, *78*, 2817–2836.

Somerville, R. C. J., and L. A. Remer (1984), Cloud optical thickness feedbacks in the CO2 climate problem, *J. Geophys. Res.*, *89*, 9668–9672.

Spencer, R. W. (1993), Global oceanic precipitation from the MSU during 1979–1991 and comparisons to other climatologies, *J. Clim.*, *6*, 1301–1326.

Tompkins, A. M. (2002), A prognostic parameterization for the subgrid-scale variability of water vapor and clouds in large-scale models and its use to diagnose cloud cover, *J. Atmos. Sci.*, *59*, 1917–1942.

Webster, P. J., and G. L. Stephens (1980), Tropical upper-tropospheric extended clouds: Inferences from winter MONEX, *J. Atmos. Sci.*, *37*, 1521–1541.

Xu, K. M., and S. K. Krueger (1991), Evaluation of cloudiness parameterizations using a cumulus ensemble model, *Mon. Weather Rev.*, *119*, 342–367.

J.-L. Lin and B. Mapes, NOAA-CIRES Climate Diagnostics Center, 325 Broadway, R/CDC1, Boulder, CO 80305, USA. (jialin.lin@noaa.gov)